Available online at www.sciencedirect.com

SciVerse ScienceDirect

Energy Procedia 37 (2013) 4457 – 4464

Energy Procedia

GHGT-11

Dissipation of overpressure into ambient mudrocks during geological carbon dioxide storage

Kyung Won Chang [a,*], Marc A. Hesse [a], Jean-Philippe Nicot [b]

[a] *Department of Geological Sciences, Jackson School of Geoscience, The University of Texas at Austin, Austin, TX 78712, USA*
[b] *Bureau of Economic Geology, Jackson School of Geoscience, The University of Texas at Austin, Austin, TX 78713, USA*

Abstract

Geological carbon dioxide (CO_2) storage in deep geological formations can only lead to significant reductions in anthropogenic CO_2 emissions if large amounts of CO_2 can be stored. Estimates of the storage capacity are therefore essential to the evaluation of individual storage sites as well as the feasibility of the technology as a whole. One important limitation on the storage capacity is the lateral extent of the pressure perturbation, the radius of review of the storage project. We show that pressure dissipation into ambient mudrocks retards lateral pressure propagation significantly and therefore increases the storage capacity. For a three-layer model of an aquifer surrounded by thick mudrocks the far-field pressure is well approximated by a single-phase model. Through dimensional analysis and numerical simulations we show that the lateral pressure propagation follows a power-law that depends on a single parameter $M \sim log_{10}(R_k R_S R_l^2)$, where R_k and R_S are the ratios of mudrock to reservoir permeability and storativity and R_l is the aspect ratio of the confined pressure plume. Both the coefficient and the exponent of the power-law are sigmoid decreasing functions of M. The M-values of typical geological storage sites are in the region where the power-law is changing rapidly. The combinations of large uncertainty in mudrock properties and the sigmoid shape lead to wide and strongly skewed probability distributions for the predicted radius of review. Therefore, the determination of the mudrock properties is an important component of the site characterization, if pressure dissipation has the potential significantly increase storage capacity. After injection the pressure will continue to diffuse and the radius of review may continue to increase, which will emphasize the significance of monitoring post-injection overpressure to secure the stability of the storage formation.

Selection and/or peer-review under responsibility of GHGT

Keywords: Carbon dioxide storage; Overpressure; Mudrock; Storage capacity; Radius of review; Post-injection

1. Introduction

The viability of a CO_2 storage project hinges on how much of the CO_2 can be injected into the storage formation, i.e. its storage capacity. *Thibeau and Mucha* [2011] argue that pressure buildup is the primary control on the storage capacity and the far-field pressure buildup that results from the displacement of formation fluids cannot be mitigated by the addition of injectors within the same field. Therefore, the far-field pressure perturbation may be an important constraint on the overall storage capacity and requires the definition of a radius of review r_f for a geological CO_2 storage site. *Thornhill et al.* [1982] defines the

1876-6102
Selection and/or peer-review under responsibility of GHGT
doi:10.1016/j.egypro.2013.06.350

Nomenclature

r_f	[km]	radius of review
p	[Pa]	overpressure (the amount of pore pressure exceeding the hydrostatic pressure)
c_t^i	[Pa^{-1}]	total compressibility under the condition of uniaxial stain and incompressible grains [*Van der Kamp and Gale*, 1983; *Green and Wang*, 1990]
c_r^i	[Pa^{-1}]	rock compressibility ($i = m$ for mudrock and s for sandstone)
c_f	[Pa^{-1}]	fluid compressibility ($4.0\times10^{-10}Pa^{-1}$ [*Freeze and Cherry*, 1979])
k_i	[m^2]	permeability
ϕ_i	[$\cdot$]	porosity
μ	[$Pa\ s$]	fluid viscosity
S_i	[Pa^{-1}]	uniaxial specific storage coefficient ($S = c_f\phi + c_r \approx c_r$) [*Wang*, 2000]
D_i	[m^2/s]	hydraulic diffusivity ($D = k/\mu c_t\phi$)

radius of review as the area in which injection-induced overpressure above the pressure cutoff may cause migration of the injected or pre-existing formation fluids into potable groundwater resources. *Birkholzer et al.* [2011] define the pressure cutoff as the minimum value above which the sustained migration of formation fluids into the potable aquifer is induced. On the geomechanical aspect, the hydraulic fracturing of the sealing unit can limit the maximum injection-induced overpressure ranging between 3.5 and 8*MPa/km* [*Thibeau and Mucha*, 2011]. For a typical reservoir at a depth of 1.5*km* the pressure cutoff is in the range from 0.1*MPa* to 10*MPa*, and we choose an intermediate value of 1*MPa* in the example calculations.

Commonly, CO_2 storage studies focus only on the target reservoir because low-permeability mudrocks prevent vertical CO_2 migration due to high capillary entry pressure. However, most regional aquifers are not closed and also the overlying and underlying mudrocks are not perfectly impervious [*Neuzil*, 1994; *Dewhurst et al.*, 1999], and pressure buildup caused by injection may partially dissipate into and through these units. The vertical pressure communication between layers mostly depends on the vertical permeability and storativity of the seals [*Domenico and Schwartz* 1998; *Hovorka et al.*, 2001; *Hart et al.*, 2006; *Zhou et al.*, 2008; *Birkholzer et al.*, 2009; *Chadwick et al.*, 2009].

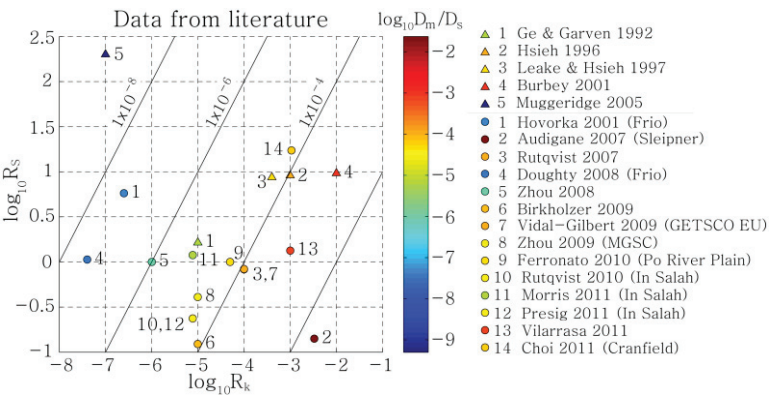

Figure 1. The data of R_k and R_S from the previous studies of pressure diffusion in a layered system for hydraulic pumping and geological CO_2 storage. The diagonal lines represent the same ratio of hydraulic diffusivities D_m/D_s

Figure 1 shows the values of R_k and R_S used in the previous studies of hydraulic pumping and CO_2 storage. We can see that the ratios R_k and R_S for CO_2 storage sites vary by 6 and 3 orders of magnitudes respectively. This suggests that current CO_2 injection sites shown in Figure 1 span the range of almost no dissipation of overpressure to a considerable dissipation into the mudrocks and may undergo a large range of possible reservoir responses to injection-induced overpressure. The effect of mudrocks, however, on the lateral pressure propagation in the storage remains poorly understood. We perform a scaling analysis and a simulation study of the simplified layered model to provide a pressure history. This study aims to quantify the effect of pressure dissipation into ambient mudrocks on

the lateral pressure propagation, the radius of review, and the storage capacity as a function of the petrophysical parameters of both layers, the thickness of the reservoir, and the injection rate and duration.

2. Model problem

We focus on far-field pressure necessary to define the radius of review. *Nicot et al.* [2009] argues that at late times and large distances the pressure disturbance created by the single and two-phase injection will be similar, and therefore we can use the single-phase pressure in this study.

2.1. Governing equation

Chang et al. [201x] describe the governing equation and the scaling analysis for pressure diffusion in a layered system. They shows that the pressure propagation within the reservoir surrounded by permeable and compressible mudrocks is governed by three independent governing dimensionless parameters defined as

$$R_k = \frac{k_m}{k_s},\ R_S = \frac{S_m}{S_s},\ R_l = \frac{r_c}{z_c} = \frac{\sqrt{D_s \Delta t}}{H_s}. \tag{1}$$

In heterogeneous media, the one-dimensional pressure diffusion equation, in which we can define hydraulic diffusivity D, cannot be rearranged to introduce $D_m/D_s \sim R_k/R_S$ as a dimensionless parameter.

Table 1. Summary of Model Properties

	Properties		Figures 2	Figure 3
Mudrock	k_m	[m^2]	Var.[a]	Var.
	c_r^m	[Pa^{-1}]	1.22×10^{-8}	Var.
	ϕ_m	[·]	0.35	0.35
	H_m	[m]	3000	3000
	L	[m]	10000	10000
Sandstone	k_s	[m^2]	5.43×10^{-14}	5.43×10^{-14}
	c_r^s	[Pa^{-1}]	6.15×10^{-10}	6.15×10^{-10}
	ϕ_s	[·]	0.25	0.25
	H_s	[m]	25	10, 25, 50, 75, 100
	L	[m]	10000	10000
Fluid	c_f	[Pa^{-1}]	4×10^{-10}	4×10^{-10}
	μ	[Pa s]	1×10^{-3}	1×10^{-3}

[a] If a parameter was varied systemically, it is indicated by "Var.", and given in the legend or axes of the respective figure.

The model properties are summarized in Table 1, and the reference cases for the application of the results are defined using physical properties from the CO_2 injection sites: In Salah (Krechba, Algeria), Frio (TX, USA), and Cranfield (MS, USA). We do not reproduce the particular conditions at these sites, and therefore we refer to them below as In Salah-type, Frio-type, and Cranfield-type sites or reservoirs.

2.2. Limiting radial solution

If $\tilde{r}_w$ and either R_k or R_l approaches zero, the problem reduces to the solution of *Thesis* [1935]. Previous studies of pressure diffusion have suggested that the self-similarity between r and t can explain the propagation of the pressure front in the radial semi-infinite domain [*Van Poolen*, 1964; *Talwani and Acree*, 1984]. The radial distance to the pressure front from a source, the radius of review, is given by

$$\tilde{r} = \delta\sqrt{t}, \qquad \delta = \exp\left[-\frac{\Delta p}{p_c} + \frac{0.80907}{2}\right]. \tag{2}$$

In the limit of $\Delta p/p_c \le 0.05$ the coefficient δ approaches 1.5 at which $\Delta p/p_c$ is not considered to be an independent parameter. Below we show that dissipation into ambient mudrocks affects this first order

scaling-law for the lateral propagation of the pressure pulse. Although the propagation follows a power-law in all cases, the coefficient δ and more importantly the exponent decreases with increasing dissipation.

3. Numerical results

We performed numerical simulations of the model using numerical grids that are highly refined near the boundary of the reservoir as shown in Figure 2(a) to resolve the strong pressure gradient typical for this problem, as in the pressure field shown in Figure 2(b). Before considering the full problem governed by all three parameters, we illustrate the effect of pressure dissipation on the power-law by varying R_k while keeping R_S and R_l fixed. Figure 2(c) shows how increasing mudrock permeability allows pressure dissipation and reduces the speed of lateral pressure propagation. To quantify these dissipative losses, we assume a general power-law for the pressure propagation as

$$\tilde{r}_f = \alpha \tilde{t}^{\beta} . \quad (3)$$

The coefficient α and the exponent β are functions of R_k, R_S, and R_l. In the limit of impermeable surrounding layers, β approaches 0.5 and α approaches δ. To analyze the effect of each parameter on the pressure evolution, we performed 480 simulations for a parameter study varying R_k from 10^{-8} to 10^{-2}, R_S from 10^0 to 10^2, and R_l from 10^2 to 10^3. We define the location of the pressure front using a pressure cutoff $\Delta p/p_c \sim 0.01$ so that $\delta \sim 1.5$. Both α and β decrease with increasing R_k, R_S, and R_l because the attenuation of overpressure is due to either the high permeability of the mudrock (large R_k) or the high storativity of the mudrock (large R_S) or due to a large aspect ratio of pressure plume and hence a large surface area across which overpressure can leak into the mudrock (large R_l). Figure 3 shows that the contour surfaces of both α and β form a set of parallel planes in the three-dimensional logarithmic parameter space, which implies that the power-law for pressure propagation depends on a single dissipation parameter defined by the normal to these planes. The normal (n_k, n_S, n_l) is (0.41, 0.41, 0.82). We define a dissipation parameter M that will collapse the three variables into a single one:

$$M = n_k \log_{10}(R_k R_S R_l^2) - (n_k x_0 + n_S y_0 + n_l z_0) , \quad (4)$$

where (x_0, y_0, z_0) is the arbitrary origin set to the minimum values of the governing parameters (-8, 0, 2) in this study. Figure 4(a) and (b) show that all data for α and β collapse to a single line if plotted as a function of M, and are monotonically decreasing functions of M. Two plateaus where the power-law is a weak function of M are separated by a sharp transition between M of 1.5 and 4.

4. Application and discussion

4.1. Estimating the radius of review and the storage capacity

Sample calculations of the radius of review are performed for CO_2 injection with constant rate of $10Mt$ of CO_2 per year for 30 years, assuming CO_2 density ρ_g is $600kg/m^3$ at $P = 16MPa$ and T = 60 $^{\circ}C$ [*Bachu*, 2003]. Using the data of each reservoir and the information of the injection operation as shown in Table 3, we can evaluate the M-value using equation (4) as well as α and β. Then the radius of review is given by

$$r_f = \alpha(M) r_c \left(\frac{t}{t_c} \right)^{\beta(M)} . \quad (5)$$

The Theis solution (2) gives the upper limit of the radius of review, $r_{f,max}$, which regards ambient mudrocks as perfectly closed boundaries. If pressure dissipation into the ambient mudrock is included, the use of $r_{f,max}$ overestimates the radius of review up to 25% for a In Salah-type reservoir and 58% for a Frio-type one. The Cranfield-type reservoir surrounded by highly permeable and compressible mudrocks results in a large reduction of the radius of review, which may require nonlinear geomechanical models

that account for changes in storativity with increasing deformation. Even in the first two cases, the reduction in the radius of review is large enough to significantly increase the storage capacity.

Solving the following nonlinear equation, we can estimate the maximum injection period t_{max} at which the pressure front approaches the given $r_{f,max}$ and the amount of injected CO_2 G_{inj} [Gt] given by

$$\frac{r_{f,\max}}{\alpha(M(t_{\max}))} - \sqrt{D_s t_{\max}} = 0, \qquad G_{inj} = 2Q\rho_g t_{\max}. \tag{6}$$

The results confirm that permeable and compressible mudrocks provide a larger storage capacity of the reservoir. The In Salah-type reservoir with the lowest M-value is the least affected by the ambient mudrocks, but the storage capacity is reduced by 46%, if an impermeable and incompressible mudrock is assumed. For a reservoir with a larger M-value, the assumption of incompressible mudrocks underestimates the storage capacity up to 74% for a Frio-type reservoir

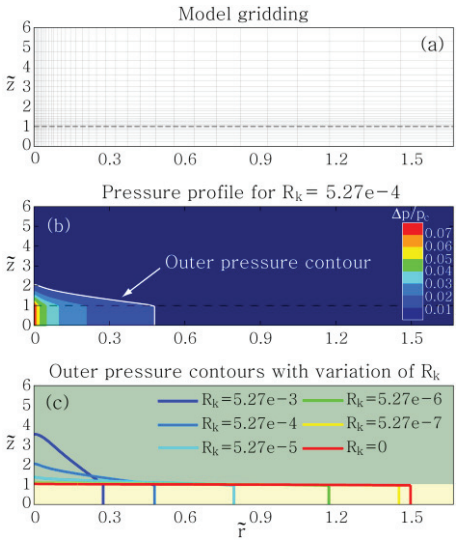

Figure 2. Figure (a) shows a typical simulation grid used in this study. Figure (b) shows a pressure profile for the case of R_k = 5.27×10^{-4}. The white line represents the pressure contour line of 1Pa of Δp ($\Delta p/p_c \sim 0.01$). Figure (c) shows that pressure contour lines corresponding to different R_k, while fixing $log_{10}R_S = 1.24$ and $log_{10}R_l = 2.55$. An impermeable mudrock ($R_k = 0$) confines injection-induced overpressure perfectly within the sandstone reservoir, and hence r_f approaches 1.5 shown as a red line.

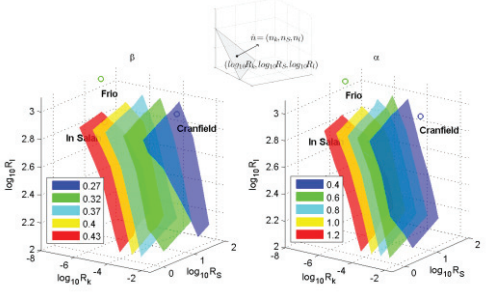

Figure 3. The variation of the power-law exponent β and coefficient α in the three dimensional parameter space.

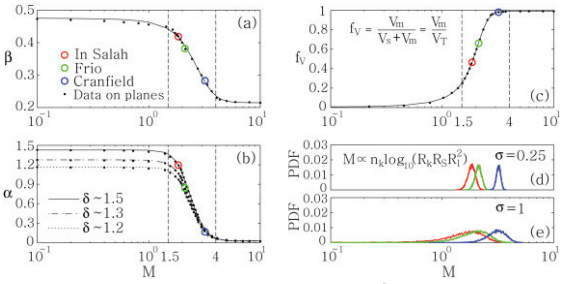

Figure 4. Figure (a) and (b) show that both β and α are decreasing functions of M. The maximum of α varies depending on $\Delta p/p_c$. Figure (c) shows f_V using equation (8). Figure (d) and (e) show the distribution of the probability density function of M.

4.2. Uncertainty due to mudrock properties

Figure 4 shows that the M-values for all three sites are in the transition region ($1.5 \leq M \leq 4$). The combination of the large variability in the mudrock properties illustrated in Figure 1 with the sensitive dependence of the power-law on M introduces large uncertainty to any estimate of the radius of review and the storage capacity. To illustrate this uncertainty, we generate 4000 values of k_m and S_m from a log-normal distribution around the preferred values with a standard deviation of either 0.25 or 1. The resulting distributions of M-values (M-distribution) are shown in Figures 4(d) and (e). The top row of Figure 5 shows the distributions of the predicted radius of review (r_f-distribution), given a fixed injection volume and injection rate. The location of the M-distribution relative to the transition zone of the sigmoidal curves for α and β determines the range and the skew of the r_f-distribution. The distribution

becomes wider but it is shifted as the variance in the mudrock properties increases. For the same variance in mudrock properties the uncertainty in the r_f -prediction is larger for the Frio-type site, because the M-distribution is located in the center of the transition zone where the power-law for the lateral pressure propagation is a strong function of M. The bottom row of Figure 5 shows the distributions of the predicted storage capacity (G_{inj} -distribution), given a fixed radius of review and a fixed injection rate. The shape of the G_{inj} -distribution depends on the solutions of the nonlinear equation (6) and is more difficult to interpret. Again the uncertainty in the $G_{in\,j}$-estimate increases with increasing variance in mudrock properties making uncertainty for the Frio-type site higher. Both of the distributions are centered on the mean and strongly skewed towards higher values.

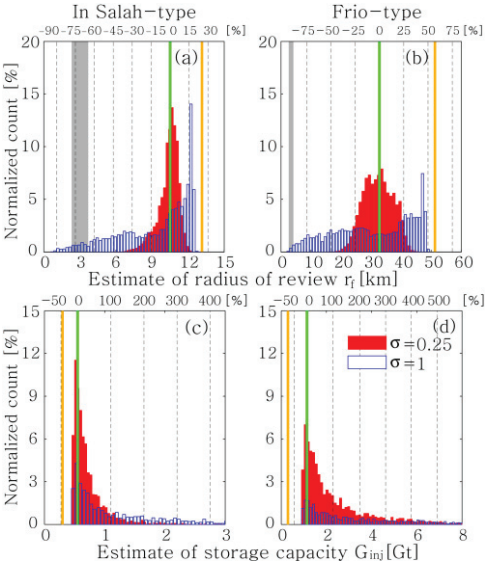

Figure 5. The effect of the uncertainty in the mudrock properties (R_k and R_S) on r_f and G_{inj}

This simple analysis illustrates the complexity in estimating the uncertainty of the radius of review or the storage capacity. In particular, estimates based on the mean physical properties of the mudrock may be good guide, if the storage capacity has to be evaluated for a given radius of review, because the maximum of the G_{inj} -distribution is close to the estimate based on the mean. In contrast, estimates based on the mean physical properties of the mudrock may not be a good guide, if the radius of review has to be evaluated for a desired storage capacity and if the uncertainty in mudrock properties is large, because the maximum of the r_f -distribution may be unrelated to the mean estimate.

4.3. Volume of the displaced fluid due to injection

The injection of CO_2 causes an increase in the storage formation pressure which will induce the displacement of the pre-existing brine in the formation as well as leakage of the brine into the ambient mudrock. In our single-phase flow model, we can calculate the amount of the fluid in each layer using following equations

$$V_s = 2\pi\phi_s c_t^s \int_0^{H_s}\int_0^{\infty} prdrdz\,, \qquad V_m = 2\pi\phi_m c_t^m \int_{H_m}^{\infty}\int_0^{\infty} prdrdz\,, \tag{7}$$

where V_i [m^3] is the volume of the fluid. The volume fraction of the total injected fluid that has been displaced into the mudrock f_V [·] is given by

$$f_V = \frac{V_m}{V_s + V_m} = \frac{V_m}{V_T}\,. \tag{8}$$

Figure 4(c) shows that f_V data also collapse into a single line as a function of M. The value of f_V increases with M because more fluids will be displaced into more permeable (larger R_k) and more compressible (larger R_S) mudrocks surrounding a thinner reservoir (larger R_l).

4.4. Evolution of post-injection pressure

The pause of CO_2 injection will cause injection-induced overpressure diffuse throughout the whole reservoir. Therefore, the radius of review may continue to increase even after the end of injection. Figure 6 shows the propagation of the far-field pressure front during and after injection with time.

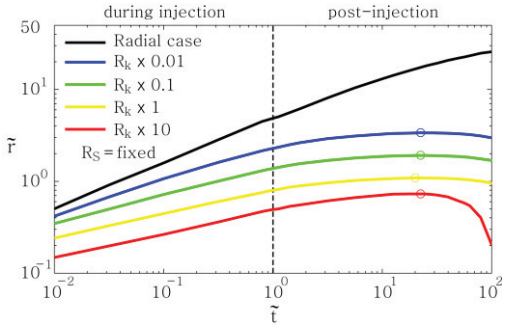

Figure 6. The location of the pressure front during and after injection. We vary only R_k and the time to pause the injection is indicated by a dash line.

During injection (left side of Figure 6), the pressure front propagates with the power-law. After injection (right side of the Figure 6), the pressure front within the sandstone reservoir propagates further up to 32% and requires 20 times more time to reach the maximum radius of review. This result implies that the monitoring of injection-induced overpressure after the injection operation is essential to secure the stability of the storage formation. As show in Figure 6, more permeable mudrocks reduce the radius of review up to 96% due to the dissipation of more overpressure into the mudrock, which implies that we need to characterize the ambient mudrock carefully to determine the threshold pressure for the failure of the formation.

Table 2. Estimates of the Radius of Review and the Storage Capacity

	Properties		In Salah-type	Frio-type	Cranfield-type
Dimensionless parameter	$log_{10}R_k$		-5.1	-6.6	-3.0
	$log_{10}R_S$		0.1	0.8	1.2
	$log_{10}R_l$		2.8	3.4	2.8
	M		1.85	2.12	3.19
	δ		1.5	1.3	1.2
Power-law parameter	β		0.41	0.38	0.28
	α		1.19	0.84	0.17
Physical properties	H_s [a]	$[m]$	12	15	32
	D_s	$[m^2/s]$	8.2×10^{-2}	1.5×10^{0}	3.8×10^{-1}
Radius of review	$r_{f,max}$ [b]	$[km]$	13.2 (+25.2%) [c]	51.3 (+58.4%)	23.1 (+632.5%)
	r_f	$[km]$	10.51	32.36	3.15
Storage capacity	$G_{inj,min}$ [b]	$[Gt]$	0.3 (−45.5%) [c]	0.3 (−74.3%)	0.3 (−99.9%)
	t_{max}	$[yrs]$	55.1	136.8	33153.4
	G_{inj}	$[Gt]$	0.55	1.17	331.53

[a] Data from *Michael et al.* [2010]
[b] Either estimates using the radial solution (2) and 10Mt/yr injection rate for 30yrs (Δt (t_{max})) excluding the ambient rock.
[c] The percentage error of $r_{f,max}$ and $G_{inj,min}$ from the preferred value r_f and G_{inj}.

5. Conclusions

This study shows that the lateral propagation of the overpressure due to CO_2 injection is significantly reduced by dissipation into ambient mudrocks. Numerical simulations show that the lateral spreading of the pressure front with time in the sandstone reservoir follows a power-law even with attenuation of overpressure into the ambient mudrock. The coefficient α and the exponent β in the power-law are governed by a single dissipation parameter $M \sim log_{10}(R_k R_S R_l^2)$. Both α and β are sigmoid decreasing function of M. The ratio of hydraulic diffusivities $D_m/D_s \sim R_k/R_S$ does not describe the lateral pressure propagation in a layered system.

A compilation of physical mudrock properties used in recent studies of geological CO_2 storage shows large variability in the three governing parameters and hence in the dissipation parameter M. The M-values of typical geological storage sites are in the region where the power-law is changing rapidly. In combination with large uncertainty in mudrock properties this leads to wide and strongly skewed probability distributions for the predicted radius of review and storage capacity. Therefore, the characterization of the physical properties of the mudrock is an important component of the evaluation of a geological CO_2 storage site.

After the end of injection, the injection-induced overpressure will continue to diffuse, which may continue to increase the radius of review. More dissipation of overpressure into mudrocks will reduce the maximum radius of review. Therefore, the effect of pressure dissipation into the ambient mudrocks should be considered in simulation studies of geological CO_2 storage that aim to determine the pressure evolution during as well as after injection.

Acknowledgements

This work is supported by the Gulf Coast Carbon Center, Bureau of Economic Geology, The University of Texas at Austin and the SECARB project, managed by the Southern States Energy Board and funded by the U.S. Department of Energy, NETL under contract number DE-FC26-05NT42590.

References

[1] Thibeau, S. And V. Mucha, Have we overestimated saline aquifer CO_2 storage capacities?, Oil & Gas Sci. Tech. Rev. IFP Energ. Nouvelles 2011; **66**, p. 81-92.

[2] Thornhill, J.T., T.E. Short, and L. Silka, Application of the area of review concept, Ground Water 1982; **20(1)**, p. 32-38.

[3] Van der Kamp, G. and J.E. Gale, Theory of earth tide and barometric effect in porous formations with compressible grains, *Water Resour. Res.* 1983; **19(2)**, p. 538-544.

[4] Green, D.H. and H.F. Wang, Specific storage as a poroelastic coefficient, *Water Resour. Res.* 1990; **26(7)**, p. 1631-1637.

[5] Freeze, R.A. and J.A. Cherry, Groundwater, Prentice Hall; 1979.

[6] Birkholzer, J.T., J.-P. Nicot, C.M. Oldenburg, Q. Zhou, S. Kraemer, and K. Bandilla, Brine flow up a well caused by pressure perturbation from carbon sequestration: static and dynamic evolutions, Int. J. Greenh. Gas Cont. 2011; **5(4)**, p. 850-861.

[7] Neuzil, C.E., How permeable are clays and shales?, Water Resour. Res. 1994; **30**, p. 145-150.

[8] Dewhurst, D.N., Y.L. Yang, and A.C. Aplin, Permeability and fluid flow in natural mudstones, in Muds Mudstones: Physical and fluid Flow Properties, edited by A.C. Aplin et al., Geol. Soc. Spec. Publ. 1999; **158**, p. 23-43.

[9] Domenico, P.A. and F.W. Schwartz, Physical and Chemical Hydrology, John Wiley & Sons Inc;1998.

[10] Hovorka, S.D., C. Doughty, P.R. Knox, C.T. Green, K. Pruess, and S.M. Benson, Evaluation of brine-bearing sands of the Frio formation, Upper Texas Gulf Coast for geological sequestration of CO_2, Conference Proceedings, In: First National Conference on Carbon Sequestration, NETL; 2001.

[11] Hart, D.J., K.R. Bradbury, and D.T. Feinstein, The vertical hydraulic conductivity of an aquitard at two spatial scales, Ground Water 2006; **44(2)**, p. 201-211.

[12] Zhou, Q., J.T. Birkholzer, C.-F. Tsang, and J. Rutqvist, A method for quick assessment of CO_2 storage capacity in closed and semi-closed saline formations, Int. J. Greenh. Gas Con. 2008; **1(2)**, p. 626-639.

[13] Birkholzer, J.T., Q. Zhou, and C.-F. Tsang, Large-scale impact of CO2 storage in saline aquifers: a sensitivity study on the pressure response in stratified systems, Int. J. Greenh. Gas Con. 2009; **3(2)**, p. 181-194.

[14] Chadwick, R.A., D.J. Noy, and S. Holloway, Flow processes and pressure evolution in aquifers during the injection of supercritical CO_2 as a greenhouse gas mitigation measure, Petrol. Geosci. 2009; **15**, p. 59-73.

[15] Nicot, J.-P., S.D. Hovorka and J.-W. Choi, Investigation of water displacement following large CO_2 sequestration operations, Energy Procedia 2009; **1(1)**, p. 4411-4418.

[16] Chang, K.W., M.A. Hesse, and J.-P. Nicot, Reduction of lateral pressure propagation due to dissipation into ambient mudrocks during geological carbon dioxide storage, submitted to *Water Resour. Res.* (under revision)

[17] Theis, C.V., The relationship between the lowering of the Piezometric surface and the rate and duration of discharge of a well using ground water storage, Trans. Am. Geophys. Union 1935; **16**, p. 519-524.

[18] Van Poolen, H., Radius of drainage and stabilization time equations, Oil Gas J. 1964; p. 138-146.

[19] Talwani, P. and S. Acree, Pore pressure diffusion and the mechanism of reservoir-induced seismicity, Pure Appl. Geophys. 1984; **122(6)**, p.947-965.

[20] Bachu, S., Screening and ranking sedimentary basins for sequestration of CO_2 in geological media in response to climate change, Environ. Geol. 2003; **44**, p.277-289.

[21] Michael, K., A. Golab, V. Shulakova, J. Ennis-King, G. Allison, S. Sharma, and T. Aiken, Geological storage of CO_2 in saline aquifers - a review of the experience from existing storage operations, *Int. J. Greenh. Gas Con.* 2010; **5**, p. 270-280.